UNIVERSITÀ POLITECNICA DELLE MARCHE

FACOLTÀ DI INGEGNERIA

CORSO DI LAUREA MAGISTRALE **BIOMEDICAL ENGINEERING**

Shielding effectiveness of mixtures emulating different kinds of soil

Efficacia di schermatura di miscele che emulano diversi tipi di terreno

RELATORE:

Chiar.mo Prof.**Primiani Mariani Valter**

CORRELATORI:

Chiar.mo Prof. **Franco Moglie**

TESI DI LAUREA DI:

Pulukuri Lokesh

A.A. **2021 / 2022**

ACKNOWLEDGEMENT

First and foremost, I want to thank God the Almighty for seeing me through this project. Secondly, I want to express my deepest appreciation to my supervisor Primiani Mariani Valter and co-supervisors Professor Moglie Franco for his constant motivation, inspiration and, guidance throughout the journey of this study. In a special way, I want to pour out my heartfelt gratitude and appreciation to my co-supervisor Engineer Colella Emanuel. for his time, guidance, and tireless assistance while carrying out the experiments and analyzing the data for this study. This study would not have been possible. Thank you very much and may God largely reward you all. I also want to extend my gratitude to the UNIVPM fraternity for availing me the opportunity to expand my skill sets through Ersu scholarship and lastly but not the last, I want to thank my parents and family members who constantly supported me with words of encourage and prayers which saw me through this journey. Now, I desired to thank my FRIENDS, in the last two years there were a lot of changes in my life, some of them due to you. I laughed, I got angry, I cried with you and for you. Thank you to give me your best and to believe in me. Just I can say here, in black and white, is we are brothers of life and for life.

ABTRACT

In electromagnetic radiation analysis, the multiple layers act like shield can be used to carry out tests such as emission tests due to effect of electromagnetic waves passes through the outdoor environment to indoor environment, evaluation of the shielding effectiveness of various materials, and more. To ensure that the multiple layers is used correctly during tests, it is necessary to make sure that certain values of some characteristic parameters are reached. In this thesis the shielding effectiveness of various materials will be analysed using a python code analysis through as assuming the multi layers placed in walls of the living room environment and to observe the electromagnetic waves.

INDEX

LIST OF FIGURES

Chapter 1

1- Electromagnetic screens

1.1 Introduction

A system known as electromagnetic shielding can lessen the electromagnetic field produced by a source in a specific space [1].

Metal containers that entirely encapsulate an electrical gadget or a portion of it are referred to as shields. A screen performs two fundamental tasks:

- The first is to stop the equipment's electrical devices, or a compound of them, from emitting emissions that would otherwise radiate outside the equipment's container:
- The second is to stop radiated emissions from connecting with internal electronic components and interfering with their functionally.

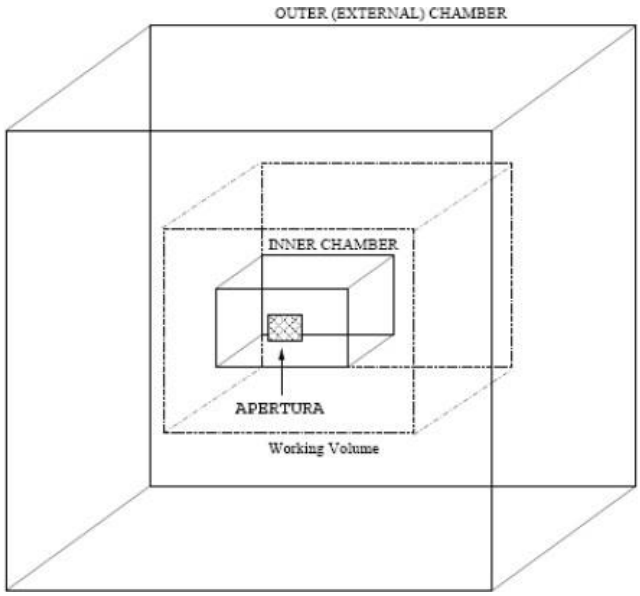

Figure 1.1: Nested chamber used as an electromagnetic shield.

Shielding can therefore be employed to lesson susceptibility to outside signals brought on by radar or powerful radio and television transmitters. A screen can theoretically be thought of as physical obstruction to the transmission of electromagnetic fields. The optimal (ideal) efficacy that can be achieved through a screen to reduce susceptibility and emission effects is only possible if the electronic devices are completely enclosed inside, and the screen has no access points from the

outside, such as openings, joints, slots, or cables. This makes inserting a screen to achieve this goal not always as simple. If not properly protecte

d, any access point through a screen could have a significant impact on how effective it is. Consider a shield, which is a closed metal box, into which a wire is inserted. If an antenna emits an electromagnetic field nearby, this field couples with the wire to produce an induced current, which flows freely through the shield and couples with the electronics inside. The converse can also happen, i.e., the system's internal disturbance partners with the wire that exits to the outside and radiates. This eliminates the protective effect. The passing of a wire via the shield must be properly handled if the shield is to remain effective. One of the most popular techniques is to attach filters to the cable at the location where the shield crosses it. Another technique is to utilize shielding cables, whose shield is connected to the equipment's shield all the way around.

This is due to the possibility of currents caused by external fields if the cable screen is linked to the device screen via a different wire. Currents that are present on the cable shield may be carried to the inner surface of the equipment shield, where they may radiate once more to the internal electronic devices, decreasing the shielding efficacy of the apparatus. The interference currents that are present on the shield's internal surface have the potential to exit along the cable shield's external surface and radiate from there. Additionally, the cable shield needs to be connected to a point of zero potential to achieve a shield that effectively lowers a cable's radiated emissions (ideal ground).

1.2 Shielding effectiveness

The shielding effectiveness of a screen is defined as the ratio between the incident electric (or magnetic) field without the screen and the incident electric (or magnetic) field with the screen present [1].

In terms of the electric field:

$$\frac{SEE = 20\log 10|E0|}{|Es|} \tag{1.1}$$

In terms of magnetic field:

$$\frac{SEH = 20\log 10|H0|}{|Hs|} \tag{1.2}$$

In terms of power:

$$\frac{SEP = 10\log 10|P0|}{|Ps|} \tag{1.3}$$

To obtain a quantitative definition, consider a metal barrier (shield) of thickness t, conductivity σ, relative electrical permittivity ε_r and relative magnetic permeability μ_r.

Suppose we have an incident wave on this barrier which will inevitably cause the presence of a reflected wave and a transmitted one.

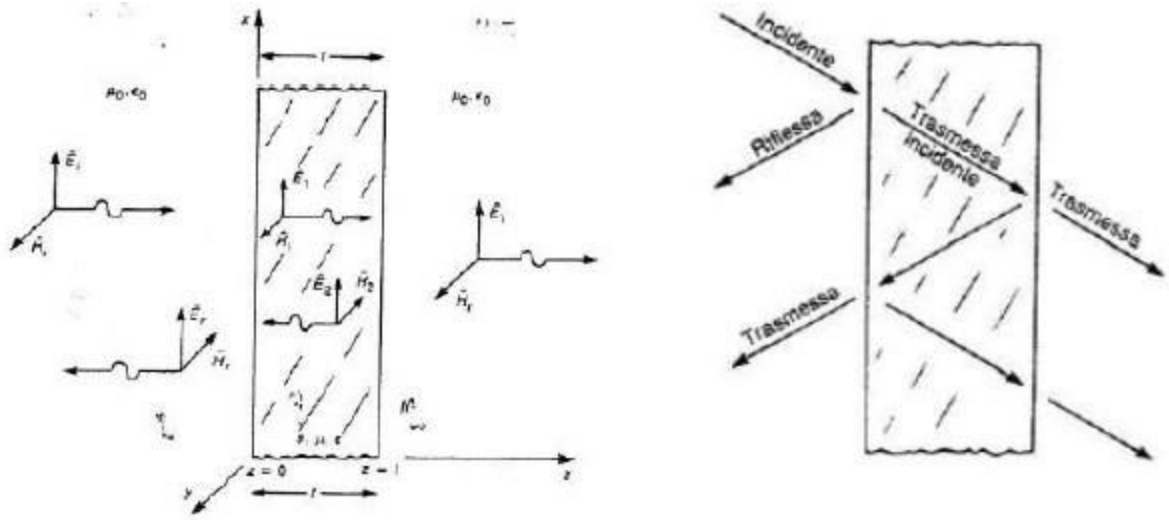

Figure 1.2 Multiple reflections in one screen

The incident field decreases during the passing of the barrier due to a variety of factors. A portion of the field is reflected, and this portion is dependent on the material's coefficient of reflection. The amplitude of the wave is reduced by a factor of $e^{-\alpha z}$, where z is the material's attenuation constant. Absorption losses are the term used to describe this occurrence. Due to the skin effect of the material, when the screen is formed of a good conductor, the attenuation constant is linked to the penetration depth as a= $\frac{1}{\delta}$. Therefore, the amplitude of the fields is attenuated according to the factor $e^{-\frac{z}{\delta}}$.

The transmitted wave overcomes the first interface and reaches the severely attenuated right-hand interface if the barrier thickness t is more than δ at the frequency of the incident wave. At the appropriate interface, a portion of the incident wave is transmitted, and a portion is reflected. Since I have a large attenuation, the effect may be ignored. The reflected component returns to the left interface and is partially transmitted there. Reflection losses are the name of this effect.

If instead the thickness t of the barrier is less than δ then the transmitted wave arrives at the right interface and represents an incident wave for the right interface. Most of this wave travels through the interface while a little portion is rejected. A component of the signal is transmitted, a portion is reflected, and a portion is returned to the left interface. The one that is mirrored goes back to the right part, and so on. The procedure remains the same, but when the consecutive portions of the reflected and transmitted field travel through the thickness is less than δ. Multiple reflections and transmissions are the term for this phenomenon.

After all of this, the expression of shielding efficiency may be broken down into three parts, each of which represents the phenomena of loss by reflection, loss by repeated reflections, and loss by absorption. If expressed in dB:

$$SE_{db} = R_{dB} + M_{dB} + A_{dB} \quad (1.4)$$

Where M stands for the additional effects of repeated, continuous reflections and transmission, A stands for the absorption losses brought on by wave propagation through the barrier, and R stands for the reflection losses brought on by reflection at the left and right interfaces.

It is noted that several reflections generate fields that combine with the initial transmitted field and lessen effectiveness. Therefore, while R and A are positive, the loss factor for many reflections M is a negative value.

1.2.1 Calculation of parameters for shielding effectiveness

The wave impedance of the material is calculated as:

$$\eta_m = \sqrt{\frac{j\omega\mu}{\sigma} + j\omega\varepsilon}$$

If then the material is

A good insulator $\eta_m = \sqrt{\frac{\mu}{\varepsilon}}$

A good conductor $\eta m = \sqrt{\frac{j\omega\mu}{\sigma}}$

If the impedance jump between the air and the material is high, the wave undergoes a strong reflection when it affects the surface. This reflection is defined by the reflection coefficient (1.5) from which the transmission coefficient (1.6) is obtained:

$$\Gamma 0 = \frac{\hat{\eta}m - \eta 0}{\hat{\eta}m + \eta 0} \quad (1.5)$$

$$To = 1 + \Gamma o = \frac{2\eta m}{\eta m} + \eta o \quad (1.6)$$

Absorption losses A_{dB} consider how the field width at the right interface is attenuated due to the thickness t of the material with respect to incident field in the left interface. This factor is described as $e^{-\frac{t}{\delta}}$. The factor of absorption is described:

$$A_{dB} = 20\log_{10} e^{\frac{t}{\delta}} \quad (1.7)$$

As far as R_{dB} reflection losses are concerned, it has been said previously that if thickness t of the material is greater than the penetration δ due to skin effect then they are possible neglect multiple reflections and consider one. Thus, the term for reflection can be schematized in this way: indicating with E0 the incident wave on the left interface and with E2 the transmitted wave after the right interface. It is then indicated with E1 the wave inside the material which is partially absorbed.
The reflection loss factor is described as:

$$R_{dB} = 20\log_{10}(|\frac{\eta m+\eta o}{4\eta m\eta o}|)^2 \quad (1.8)$$

Finally, in the extremely unlikely event that the thickness t is less than the penetration coefficient, the losses resulting from multiple reflections M_{dB} occur. In this situation, all the minor reflections must be considered, and we discover that E_2 is not provided by a single transmission but rather by a number of waves that are out of phase with one another:

$$M_{dB} = 20\log_{10}|1-\Gamma^2\, e^{-\frac{2(1+j)t}{\delta}}| \quad (1.9)$$

Summing up the three contributions we get:

$$SE_{dB} = 20log_{10}\left(\left|\frac{\eta m+\eta o}{4\eta mo}\right|\right)^2 + \log_{10}\left|1+\Gamma^2 e^{-\frac{2(1+j)t}{\delta}}\right| \quad (1.10)$$

1.3 Shielding low magnetic fields frequency

In the literature it is illustrated that in the presence of far-field sources (considered as uniform plane waves) $r \geq \frac{2d^2}{\lambda}$ (where d is the maximum size of the radiative element and λ is the length of the electromagnetic wave) the reflection loss R constitutes the shielding mechanism predominant at low frequencies while the loss for A absorption is the predominant mechanism at high frequencies [1].
Instead, as regards the presence of near-field sources:

• For electrical sources the reflection loss R is predominant at low frequencies while the absorption loss A is predominant at high frequencies.

• For sources of the magnetic type, the loss which is predominant for all frequencies is that for A absorption.

For this reason, other methods must be used to effectively screen I low frequency magnetic disturbances.
There are two basic methods of shielding against low magnetic sources frequency:

• The deflection of magnetic flux through materials with a high reluctance value (i.e., with a strong opposition to the transit of a magnetic flux).

• The generation of a counter magnetic flux which opposes the magnetic field, commonly known as the "short-circuit loop method" (it exploits Faraday's law).

In the method of diverting magnetic flux through a material which exhibits a high reluctance value (ferromagnetic material) the magnetic field will tend to focus on the high reluctance ferromagnetic path and therefore will not go to cross the inner region of the screen.

In the short-circuit loop method, a loop is used so that the field magnetic incident passes through the surface enclosed by the coil. Thus, it is induced on the coil, by Faraday's law, an induced current Iind and an associated magnetic flux ψind with a polarity or direction such as to oppose the incident magnetic field that generated it. In this way the net magnetic field near the coil is reduced.

Unfortunately, there are two factors that can reduce the effectiveness of shielding in the technique deviation of the magnetic flux, and which must be considered:

• The permeability μr of ferromagnetic materials decreases as the frequency.

• The permeability μr of ferromagnetic materials decreases as the intensity increases of the magnetic field.

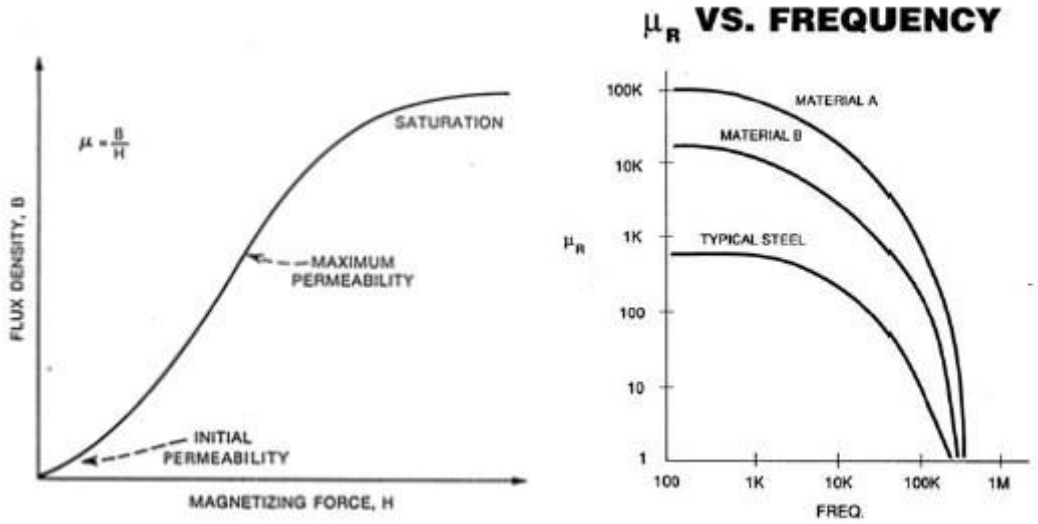

Figure 1.3 Worsening of SE due to magnetic permeability

This property makes it feasible for a material to appear to be effective at shielding low frequency fields but in practice fall short of doing so because of the intense fields when the material saturates.

A common method to minimize the effect of saturation is to use two screens:

• The first where the magnetic permeability μr is lower, and the saturation level is higher high.

• The second with a higher magnetic permeability but with a saturation level lower.

The purpose of the first layer is to reduce the magnetic field so that it fails to saturate the second screen, which has a lower saturation threshold but has a high value of μr therefore a better shielding action.

1.4 Behavior of openings

The so-called apertures that for practical purposes cannot be avoided are a prevalent entry route in real screens.

Since these openings can radiate the fields existing inside or outside of the screen, their insertion results in a significant decrease of the shielding efficiency [1]. Babinet's Principle, which asserts that the apertures can radiate like antennas whose radiating parts have the same diameters as the antenna, also describes this phenomenon. An aperture antenna is one of these. An antenna is typically described as a conducting material in which a current produces an electromagnetic field at a specific distance. Through duality, it is possible to regulate radiation that passes through metal walls that have a surface current. The moment an opening is made in this surface, the current is constrained and forced to take a different course. The radiation comes from the fissure since the opening goes to alter the current's route in some way.

This leads to the conclusion that the shape of the aperture significantly affects the quality of the radiation:

in fact, we have a much smaller deviation with a very narrow and long opening in the direction of the current than with an inverse form, that is, with a very wide and short opening in the direction of the current.

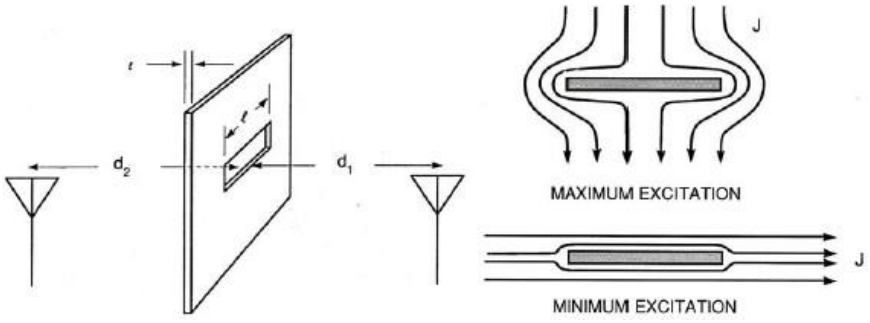

Figure 1.4 Example of minimum and maximum flow deviation

Openings can radiate as effectively as dipole antennas, according to Babinet's principle. However, it is well known that these dipole antennas perform best when their size (antenna length) is equal to half the incident electromagnetic wave's wavelength (or its multiples). The same statement is true for

an aperture if its size is half a wavelength as it becomes a very effective radiator and reduces the effectiveness of shielding. We frequently find ourselves doing compatibility tests in specialized spaces where the operators may be present for several hours but who also need access to fresh air. Waveguides, which are employed under cut, are used to provide for this. In fact, it is well known that waveguides have a cut-off frequency that varies with size below which they are unable to conduct an electromagnetic field and exhibit extremely high attenuation. Waveguides come in both circular and rectangular shapes. Further reductions in effectiveness result from the joints connecting the various components that make up the screen. For example, two parts of a container that are close to one another create an opening because, on a microscopic level, the joint contains some areas where the metals don't touch because of mechanical imperfections in the container's construction. The direction in which the shielding source is pointed is crucial when joints are present: Actually, if there is a horizontal joint and a horizontal coil within the screen, the current induced on the container will be parallel to the joint and won't be stopped by the latter, preventing radiation. In contrast, if the junction is vertical and there is a loop inside the screen, the joint disrupts the generated current and radiates. Because of this, when measuring the radiated emission with the card horizontally, you get findings that are acceptable, but when you flip the card vertically, the necessary standards are not met.

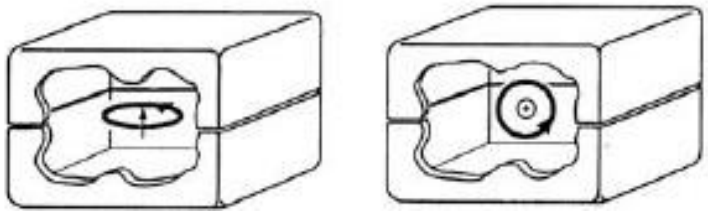

Figure 1.5 Position of the coil referred to the joint.

It should also be remembered that the joint runs the entire length of the container, making it possible to think of it as a long aperture that resonates at low frequencies. The model with a resistor and a capacitor is electromagnetically accurate enough to explain a joint:

Capacity, on the other hand, depicts the points where there is no physical contact between the two portions of the screen because of microscopic flaws, whereas resistance reflects the effective contact resistance that occurs when it is the contact. The presence of a potential difference can then be determined by defining a transfer impedance. If the joint were perfect, this stress would be zero, but the radiation caused by the joint's imperfection increases with increasing potential difference. There are many methods for lowering transfer impedance, and one of them is improving connections. For instance, screws that reduce contact resistance to extremely low levels can be employed. Increasing

the contact surface is another technique to reduce the transfer impedance and, consequently, the residual voltage inside, as the impedance depends on the contact resistance, which in turn depends on the surface as $\frac{\rho L}{S}$ where S is the surface. As the surface increases, the contact resistance decreases. In the figure 1.6 shows two examples to increase performance.

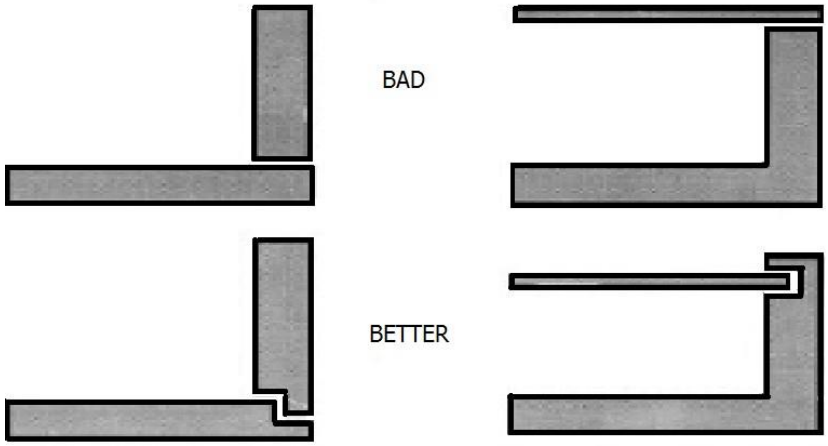

Figure 1.6 Examples for decreasing the transfer impedance.

Additionally, the contact resistance fluctuates with pressure: as you tighten the screw, the contact resistance quickly decreases and then stabilizes at a nearly constant value. To be able to tighten the screws consistently with the same pressure, torque wrenches may frequently be needed. Gaskets are used when you require even more defense. They must be composed of conductive material to ensure electrical contact between the two components. Although there are many kinds of electromagnetic seals available, coaxial cable-style metal braiding is the most popular. The gaskets are quite helpful because they help to correct any little imperfections in the mechanics between the joints. The fundamental issue is that once a gasket is installed and compressed, if it is later taken out and changed, it will no longer have the same push force. Therefore, an effort is made to make the gasket as elastic as possible by introducing rubber conductors that apply pressure between the joint's components to prevent this. These tires feature great flexibility and high conductivity due to the amalgamation of graphite, which reduces the contact resistance. Then there are the gaskets used in laboratory doors, which are constantly being opened and closed. They are made using a kind of tiny knife that presses against the slats and enters the gasket on the fixed part of the door to secure the electrical contact along the entire door. A zig-zag access path to the laboratory is erected, with the walls covered in absorbent cones that attenuate a significant portion of the incoming radiation from the outside. This

is done in case you need to keep the door of the lab open while the test is being conducted. Having said that, it is acknowledged that the pressure that the gaskets must withstand is crucial. As a result, the makers offer graphs that illustrate the trend and specify the suggested pressure range, which is between a minimum and a maximum. You must not go below the minimum value to prevent too low of a contact resistance, and you must not go above the maximum value to prevent reaching the gasket's elasticity's point of no return.

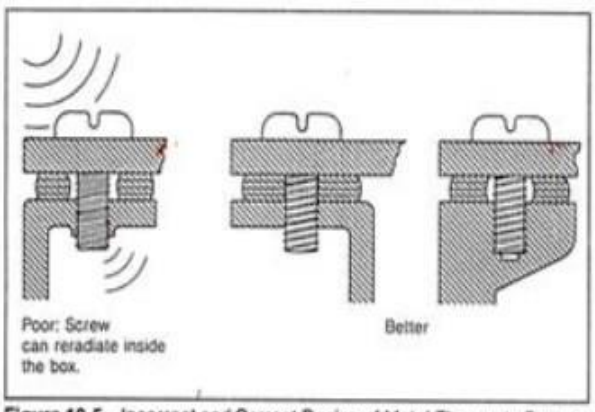

Figure 10.5—Incorrect and Correct Design of Metal Flanges to Prevent Screw-Leakage Inside the Box

Figure 1.7 Methods of screwing the screws.

The first scenario, despite being the most prevalent, is the least effective since it involves a screw being inserted into an internal L. If this happens, the field within the container may be penetrated by the screw's thread. The other two solutions, the first of which has an external L for which the screw stays outside the apparatus and the second of which always has an internal L but creates a block in which the screw is screwed in such a way that the screw remains drowned inside the block and is unable to create a field penetration inside the container, are used to solve this problem. Logically, cables like network and monitoring cables are required for communication between the insulated equipment and the outside world. Note that the cable mass is connected directly to the outer and inner surface of the screen, given that at 50 Hz (power frequency) the penetration thickness δ is large enough to allow to consider the two ground wires in contact.

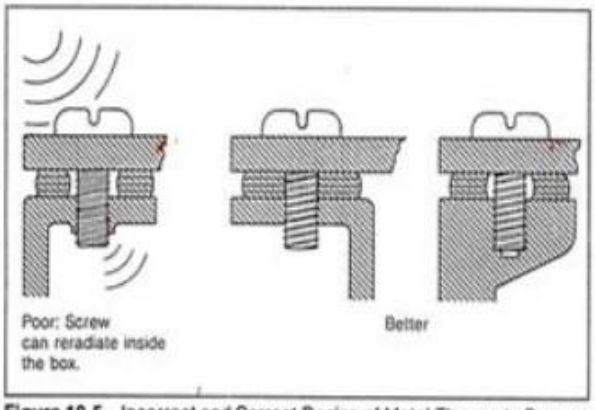

Figure 10.5—Incorrect and Correct Design of Metal Flanges to Prevent Screw-Leakage Inside the Box

Figure 1.8 Ground connection type

Regarding data transmission in both ways, inserting a capacitor to direct the disturbance current into the screen casing is the most logical way to stop disturbances. Putting the capacitor inside the screen causes the common-mode noise current to find the condenser and remain inside, not affecting the wire that comes out, which is why this solution is used for an emissions problem. Mounting the capacitor outside has a different effect than mounting it inside the screen. When the capacitor is placed outside, the disturbance is kept out and it can be used to solve a susceptibility issue. But the capacitor also exhibits behaviors that are dependent on the parasitic characteristics; for instance, if the disturbance surpasses the resonance frequency, it exhibits inductance-like behavior. A passing capacitor is employed that has an exterior hard shield made of a metal tube to solve the full set of issues. As a result, the wire that needs to be passed through has a central conductor that is attached to the outer braid. The benefit of this concentric through capability is that the metal wall's outer sheath is welded or bolted on all the way around the circumference. In this manner, one of the armatures is the wire that passes and as a result, there are no additional conductors. The other armature is directly welded to the receiver and as a result, there is no wire connecting the armature to the receiver, and as a result, the parasitic elements in this situation are essentially nonexistent. Another major benefit is that there is no field penetration because you have ground capacity for both incoming and outgoing disturbance. If just one hole is built for the passage of coaxial cables, another cable is made coaxial, with the shield of the coaxial cable serving as the inner conductor and the hole in the wall serving as the outer conductor. As a result, we have a TEM system that enables induced currents to go along the exterior of this new coaxial cable. As a result, both the use of the coaxial cable and the screen are rendered useless because the outer sock acts as an antenna to pick up the signal and transmit it within

the screen. Through welding or the use of a metal connection into which the coaxial cable is screwed, the coaxial cable must be fed through a gap between the cable screen and the metal of the wall. This keeps the current that is induced on the coaxial cable's outer braid on the outer wall.

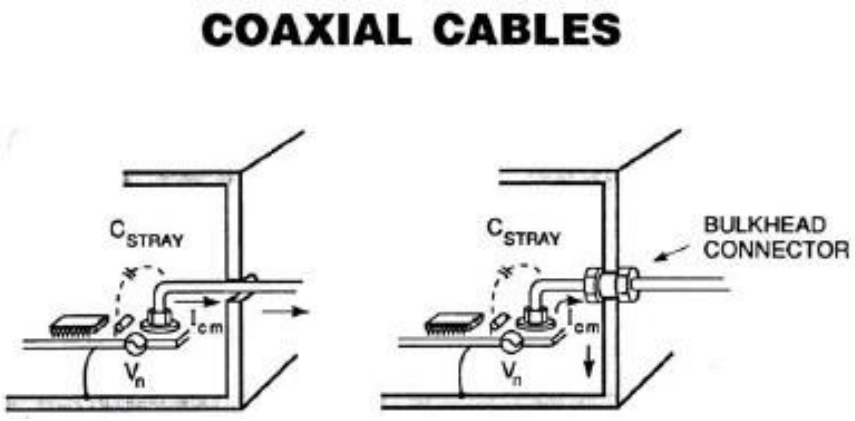

Figure 1.9 Passage of coaxial cables

Chapter 2

2. Finite-Difference Time Domain

2.1 Introduction

To determine the electromagnetic field produced by a source, one must typically turn to inhomogeneous Maxwell equations, whose resolution, save in rare circumstances, is excessively complicated [5]. They are conducted as approximations that enable their resolution using numerical techniques based on the analysis of the problem. There are various numerical techniques for computing the electromagnetic field and resolving Maxwell's equations:

• Radiated field from an antenna in zero-gravity, moments method.

• Finite difference method used to the radiation field from an antenna in the presence of complicated dielectrics.

• The field that an antenna radiates in wide areas, geometric optics.

To determine the electromagnetic field produced by a source, one must typically turn to inhomogeneous Maxwell equations, whose resolution, save in rare circumstances, is excessively complicated [5]. They are conducted as approximations that enable their resolution using numerical techniques based on the analysis of the problem. There are various numerical techniques for computing the electromagnetic field and resolving Maxwell's equations:

- Radiated field from an antenna in zero-gravity, moments method.
- Finite difference method used to the radiation field from an antenna in the presence of complicated dielectrics.
- The field that an antenna radiates in wide areas, geometric optics.
- Finite element technique

For the analysis and design of antennas, the investigation of signal propagation in semiconductor devices, the analysis of scattering and absorption scenarios, and other applications, the Finite-Difference Time-Domain (FDTD) method is used. This technique is based on the Kane Yee algorithm from 1966 [10], which is still in use today and was introduced for the first time by Taflove [6]. In essence, this approach converts all differential equations into finite differences. The technique applies this modification to the Maxwell equations in the time domain while carefully selecting the sample time step. The result is a set of linear equations in which the values of the magnetic and electric fields

at a given time and location are calculated from those of the fields at places that are near and in relation to the previously studied time step.

Six Cartesian field components are the unknowns in the FDTD's iterative technique, and they are calculated on a 3-D grid of simple cells that determine the spatial resolution. As a result, we can now track the temporal trend of the fields at any location in space.

The FDTD method has the following advantages:

- Conceptual and mathematical simplicity.
- Independence from geometry and material characteristics.
- Possibility of study over time.

On the other hand, however, it has:

- Requirement of powerful computers.
- Discretization can introduce systematic errors.
- At low frequencies, approximations must be made.

Furthermore, the FDTD algorithm lends itself very well to code parallelization, in particular way to the analysis of a reverberant room where the position of the stirrers is varied ad each step of a certain angle. By doing this, the calculation times are reduced noticeably.

Troubleshooting the FDTD involves:

- Division of the space to be studied into a grid of nodes (space, time).
- Discretization of Maxwell's equations over time.
- Solution of finite difference equations.

2.2 Yee algorithm and notation

Yee's algorithm generates a set of finite difference equations for the Maxwell system in the case of materials with small losses where $\rho = 0\ and\ \sigma = 0$. This algorithm uses both electrical and magnetic properties simultaneously to evaluate the electromagnetic field's values in both time and space. The process is divided into two parts. In the first, we discretize the structure's geometry using a 3-D lattice made up of several cubes, which establishes the spatial resolution. Yee's algorithm divides space into a three-dimensional grid, placing the magnetic fields in the center of the cube's faces and the electric fields on the cube's edges. As a result, four magnetic field components surround each electric field component, and four electric field components surround each magnetic field component. The unit cell we're referring to is seen in Fig. 2.1. Materials that absorb electromagnetic radiation with time-

independent electrical characteristics can be found in this source-free region of space. Since Faraday's and Ampère's laws are derived from Maxwell's equations in this case, it is possible to identify the electric field components by looking at the flow current connected to the circuitry of H, and the magnetic field components by looking at the magnetic flux connected to the circuit of E.

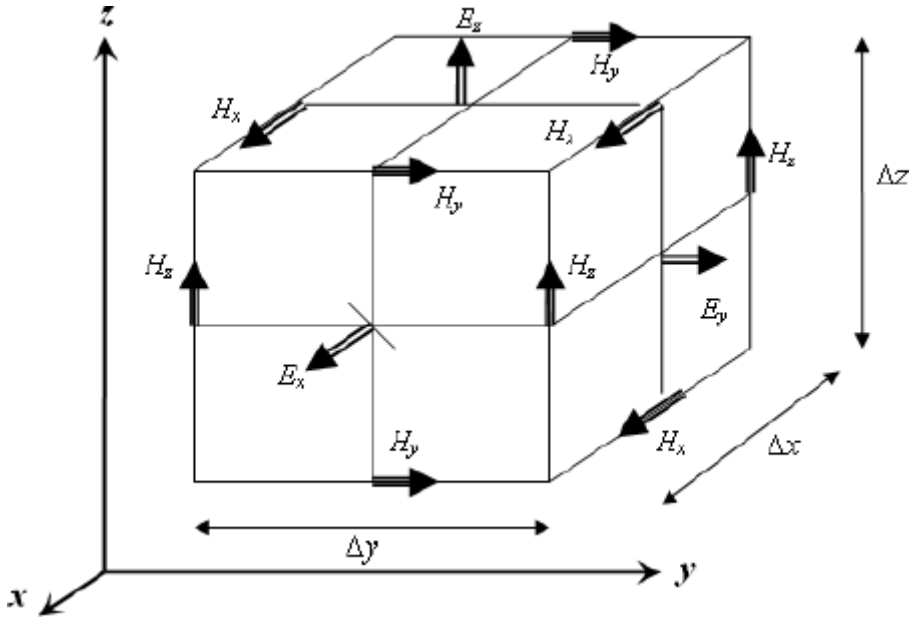

Figure 2.1 Yee lattice elementary cubic cell and its sampling points for electromagnetic fields.

To study a problem with the FDTD approach, one must specify the permittivity and the permeability of the material; in this way a stepwise approximation of the is obtained surface and internal geometry of the structure of interest. The spatial resolution is given by the size of the unit cell. Also, electric, and magnetic fields are evaluated on different time axes. Having decided the time step Δt based on stability criteria, the algorithm calculates the electric components every $n \cdot \Delta t$ and the magnetic ones every $(n+1/2) \cdot \Delta t$, with n = 1,2,3…

Looking at the example of Figure 2.2 the magnetic field components are calculated at the instant $1 \cdot \Delta t$ using those of the electric field, calculated and memorized in step previous $0.5 \cdot \Delta t$. The magnetic fields at the instant $1.5 \cdot \Delta t$ will be calculated using the previous electrical components, calculated, and memorized in the previous step $1 \cdot \Delta t$. Therefore, it creates a recursion which allows to avoid numerical problems deriving from systems of equations and matrix inversions.

The second step of the algorithm performs the transformation from partial difference equations (PDE) to finite difference equations (FDE).

Starting from system 2.1:

$$\begin{aligned}
\frac{\partial Hz}{\partial y} - \frac{\partial Hy}{\partial z} &= \varepsilon \frac{\partial Ex}{\partial t} + \sigma Ex \\
\frac{\partial Hx}{\partial z} - \frac{\partial Hz}{\partial x} &= \varepsilon \frac{\partial Ey}{\partial t} + \sigma Ey \\
\frac{\partial Hy}{\partial x} - \frac{\partial Hx}{\partial y} &= \varepsilon \frac{\partial Ez}{\partial t} + \sigma Ez \\
\frac{\partial Ey}{\partial z} - \frac{\partial Ez}{\partial y} &= \mu \frac{\partial Hx}{\partial t} \\
\frac{\partial Ez}{\partial x} - \frac{\partial Ex}{\partial z} &= \mu \frac{\partial Ey}{\partial t} \\
\frac{\partial Ex}{\partial y} - \frac{\partial Ey}{\partial x} &= \mu \frac{\partial Hz}{\partial}
\end{aligned} \tag{2.1}$$

The FDTD method allows you to write the last three equations in a form like the first ones, introducing the magnetic equivalent loss σ^*:

$$\begin{aligned}
\frac{\partial Hz}{\partial y} - \frac{\partial Hy}{\partial z} &= \varepsilon \frac{\partial Ex}{\partial t} + \sigma Ex \\
\frac{\partial Hx}{\partial z} - \frac{\partial Hz}{\partial x} &= \varepsilon \frac{\partial Ey}{\partial t} + \sigma Ey \\
\frac{\partial Hy}{\partial x} - \frac{\partial Hx}{\partial y} &= \varepsilon \frac{\partial Ez}{\partial t} + \sigma Ez \\
\frac{\partial Ey}{\partial z} - \frac{\partial Ez}{\partial y} &= \mu \frac{\partial Hx}{\partial t} + \sigma * Hx \\
\frac{\partial Ez}{\partial x} - \frac{\partial Ex}{\partial z} &= \mu \frac{\partial Ey}{\partial t} \sigma * Hy \\
\frac{\partial Ex}{\partial y} - \frac{\partial Ey}{\partial x} &= \mu \frac{\partial Hz}{\partial} \sigma * Hz
\end{aligned} \tag{2.2}$$

This phase facilitates both the computation and application of the resulting numerical scheme. Yee's notation is then presented.

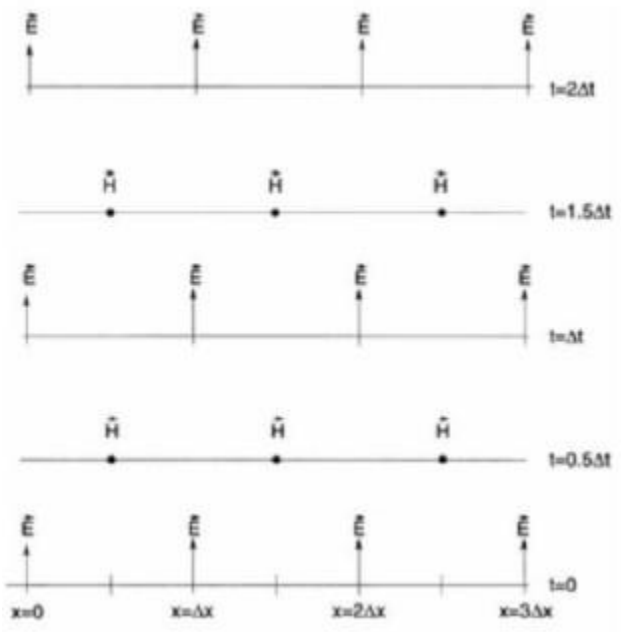

Figure 2.2 Space-time table with Yee notation for a one-dimensional plane wave. The starting fields are null in all the calculation region.

If the cell volume in Figure 2.1 is:

$$\Delta v = \Delta x \,.\, \Delta y . \Delta z \tag{2.3}$$

And the spatial discretization is uniform, it will be possible to reach each point of the lattice by varying the three indices (i,j,k) in the trio:

$$(i\Delta \mathrm{x}, \mathrm{j}\Delta \mathrm{y}, \mathrm{k}\Delta \mathrm{z}) \tag{2.4}$$

Regarding the reference system under consideration. Indices can take multiple values of ½. Initially we consider a generic function of space and time:

$$F(x, y, z, t) \tag{2.5}$$

Once the field F has been sampled in space and time, it can be represented with three subscripts (i, j, k), indicating the position in the spatial domain, and with a superscript n, denoting the instant n. Δt in which F is considered:

$$F|_{i,j,k}^{n} = F(i\Delta x, j\Delta y, k\Delta z, n\Delta t) \tag{2.6}$$

Using the notation introduced, we replace the partial derivatives of F with their incremental ratios:

$$\begin{aligned}\frac{\partial F}{\partial x} &= F_{1+i,j,k}^{\,n} - F|_{i,j,k}^{\,n} + O((\Delta x)^2)/\Delta x \\ \frac{\partial F}{\partial y} &= F_{i,1+j,k}^{\,n} - F|_{i,j,k}^{\,n} + O((\Delta y)^2)/\Delta y \\ \frac{\partial F}{\partial z} &= F_{i,j,1+k}^{\,n} - F|_{i,j,k}^{\,n} + O((\Delta z)^2)/\Delta z \\ \frac{\partial F}{\partial t} &= F_{i,j,k}^{n+1} - F|_{i,j,k}^{\,n} + O((\Delta t)^2)/\Delta t\end{aligned} \tag{2.7}$$

by discarding the terms of the second order $O\left((\Delta)^2\right)$ commits an error that does not exceed the square of the chosen increment, accuracy of the second order. If $\Delta x, \Delta y \; and \; \Delta z$ are non-homogeneous, the error drops to the first order. Yee notation allows you to have an immediate correspondence between physical variables and computer variables. Consider, for example, the fourth equation of system 2.2

$$\frac{\delta Ey}{\delta z} - \frac{\delta Ee}{\delta y} = \mu \frac{\delta Hx}{\delta t} + \sigma * Hx \tag{2.8}$$

Proceeding in the substitution of partial derivatives in space and time calculated at a point (i, j, k) in the grid with finite differences we get:

$$\frac{1}{\mu i,j,k}(Ey|_{i,j,k+\frac{1}{2}}^{\,n} - Ey|_{i,j,k-\frac{1}{2}}^{\,n}/\Delta z) - (Ey|_{i,j+\frac{1}{2},k}^{\,n} - Ey|_{i,j-\frac{1}{2},k}^{\,n}/\Delta y) - (\sigma * i,k,jHx|_{i,j,k}^{n+\frac{1}{2}}) = \frac{Hx|_{i,j,k}^{n+\frac{1}{2}} - Hx|_{i,j,k}^{n-\frac{1}{2}}}{\Delta t} \tag{2.9}$$

Field components are evaluated for the left member at time n. Instead, a magnetic field $Hx|_{i,j,k}^{n+\frac{1}{2}}$,can be seen in the right member, not stored in memory but is approximal using a semi-implicit method.

$$Hx|_{i,j,k}^{\,n+\frac{1}{2}} = \frac{Hx|_{i,j,k}^{n+\frac{1}{2}} - Hx|_{i,j,k}^{n-\frac{1}{2}}}{2} \tag{2.10}$$

Substituting equation 2.9 yields:

$$Hx|_{i,j,k}^{\,n+\frac{1}{2}} = \left(\frac{1-\frac{\sigma * i,j,k\Delta t}{2\mu i,j,k}}{1+\frac{\sigma * i,j,k\Delta t}{2\mu i.j.k}}\right)Hx|_{i,j,k}^{\,n-\frac{1}{2}} + \left(\frac{\frac{\Delta t}{\mu i,j,k}}{1+\frac{\sigma * i,j,k\Delta t}{2\mu i,j,k}}\right)((Ey|_{i,j,k+\frac{1}{2}}^{\,n} - Ey|_{i,j,k-\frac{1}{2}}^{\,n}/\Delta z) - (Ez|_{i,j+\frac{1}{2},k}^{\,n} - Ez|_{i,j-\frac{1}{2},k}^{\,n}/\Delta y)) \tag{2.11}$$

Similarly, the other components are derived:

$$Hy|_{i,j,k}^{n+\frac{1}{2}} = \left(\frac{1-\frac{\sigma*i,j,k\Delta t}{2\mu i,j,k}}{1+\frac{\sigma*i,j,k\Delta t}{2\mu i.j.k}}\right)Hy|_{i,j,k}^{n-\frac{1}{2}} + \left(\frac{\frac{\Delta t}{\mu i,j,k}}{1+\frac{\sigma*i,j,k\Delta t}{2\mu i,j,k}}\right)\left(\left(Ez|_{i+\frac{1}{2},j,k}^{n} - Ez|_{i-\frac{1}{2},j,k}^{n}/\Delta x\right) - \left(Ex|_{i,j,k+\frac{1}{2}}^{n} - Ex|_{i,j,k-\frac{1}{2}}^{n}/\Delta z\right)\right)$$

(2.12)

$$Hz|_{i,j,k}^{n+\frac{1}{2}} = \left(\frac{1-\frac{\sigma*i,j,k\Delta t}{2\mu i,j,k}}{1+\frac{\sigma*i,j,k\Delta t}{2\mu i.j.k}}\right)Hz|_{i,j,k}^{n-\frac{1}{2}} + \left(\frac{\frac{\Delta t}{\mu i,j,k}}{1+\frac{\sigma*i,j,k\Delta t}{2\mu i,j,k}}\right)\left(\left(Ex|_{i,j+\frac{1}{2},k}^{n} - Ex|_{i,j-\frac{1}{2},k}^{n}/\Delta y\right) - \left(Ey|_{i+\frac{1}{2},j,k}^{n} - Ey|_{i-\frac{1}{2},j,k}^{n}/\Delta x\right)\right)$$

(2.13)

$$Ex|_{i,j,k}^{n+\frac{1}{2}} = \left(\frac{1-\frac{\sigma*i,j,k\Delta t}{2\varepsilon i,j,k}}{1+\frac{\sigma*i,j,k\Delta t}{2\varepsilon,j,k}}\right)Ex|_{i,j,k}^{n-\frac{1}{2}} + \left(\frac{\frac{\Delta t}{\varepsilon i,j,k}}{1+\frac{\sigma*i,j,k\Delta t}{2\varepsilon i,j,k}}\right)\left(\left(Hz|_{i,j+\frac{1}{2},k}^{n+\frac{1}{2}} - Hz|_{i,j-\frac{1}{2},k}^{n+\frac{1}{2}}/\Delta y\right) - \left(Hy|_{i,j,k+\frac{1}{2}}^{n+\frac{1}{2}} - Hy|_{i,j,k-\frac{1}{2}}^{n+\frac{1}{2}}/\Delta z\right)\right)$$

(2.14)

$$Ey|_{i,j,k}^{n+\frac{1}{2}} = \left(\frac{1-\frac{\sigma*i,j,k\Delta t}{2\varepsilon i,j,k}}{1+\frac{\sigma*i,j,k\Delta t}{2\varepsilon,j,k}}\right)Ey|_{i,j,k}^{n-\frac{1}{2}} + \left(\frac{\frac{\Delta t}{\varepsilon i,j,k}}{1+\frac{\sigma*i,j,k\Delta t}{2\varepsilon i,j,k}}\right)\left(\left(Hx|_{i,j,k+\frac{1}{2}}^{n+\frac{1}{2}} - Hx|_{i,j,k-\frac{1}{2}}^{n+\frac{1}{2}}/\Delta z\right) - \left(Hz|_{i+\frac{1}{2},j,k}^{n+\frac{1}{2}} - Hz|_{i+\frac{1}{2},j,k}^{n+\frac{1}{2}}/\Delta x\right)\right)$$

(2.15)

$$Ez|_{i,j,k}^{n+\frac{1}{2}} = \left(\frac{1-\frac{\sigma*i,j,k\Delta t}{2\varepsilon i,j,k}}{1+\frac{\sigma*i,j,k\Delta t}{2\varepsilon,j,k}}\right)Ez|_{i,j,k}^{n-\frac{1}{2}} + \left(\frac{\frac{\Delta t}{\varepsilon i,j,k}}{1+\frac{\sigma*i,j,k\Delta t}{2\varepsilon i,j,k}}\right)\left(\left(Hy|_{i+\frac{1}{2},j,k}^{n+\frac{1}{2}} - Hy|_{i-\frac{1}{2},j-\frac{1}{2},k}^{n+\frac{1}{2}}/\Delta x\right) - \left(Hx|_{i,j+\frac{1}{2},k}^{n+\frac{1}{2}} - Hx|_{i,j-\frac{1}{2},k-}^{n+\frac{1}{2}}/\Delta y\right)\right)$$

(2.16)

For components E_x, E_y, and E_z the term $\sigma E^{n+\frac{1}{2}}$ due to losses state appraised using due to losses was evaluated using a semi-implicit procedure like 2.10. The equations 2.11, 2.12, 2.13, 2.14, 2.15 and 2.16 allow the values of electric and magnetic fields to be derived at any point on the grid, starting from the previous values of their scalar components and from the previous values of the dual field components on adjacent points. So, once you know the starting field, with the notation of Yee it is possible to derive the values of the fields one point at a time until you get to calculating the values of the field of the entire defined region.

2.3 Numerical dispersion and stability

The FDTD technique generates a zone of empty space where the simulated waves scatter. The numerical modes' phase velocity changes as a result, and this variation with respect to c relies on the grid's wavelength and propagation direction. If the spatial resolution rises, the numerical dispersion will also fall. The waves don't move in actual space; instead, they do so in a numerical "space" that introduces delays and has the potential to introduce phase problems. Waveforms in this area are prone to distortion, anisotropy, and instances of pseudo-rephrazion. Knowing the boundaries of FDTD modeling is fundamentally influenced by this numerical dispersion, particularly when working with electrically massive systems. Consider a region of free space normalized to c by imposing $\mu = 1$, $\varepsilon = 1$, $\sigma = 0$, $and\ \sigma^{*} = 0$ Combining the rotor equations and introducing a complex vector. $V = H + lE$ we reach:

$$l\nabla * \mathrm{V} = \frac{\delta \mathrm{V}}{\delta \mathrm{t}} \tag{2.17}$$

Substituting the field vector within the space-time realization of yields:

$$\left[\frac{x}{\Delta x}\sin(\frac{\mathrm{k^{x\Delta x}}}{2}) + \frac{y}{\Delta y}\sin\left(\frac{\mathrm{k^{y\Delta y}}}{2}\right) + \frac{\mathrm{z}}{\Delta z}\sin\left(\frac{\mathrm{k^{z\Delta z}}}{2}\right)\right] * V\Big|_{i,j,k}^{n} = \frac{-\mathrm{l}}{\Delta t}V\Big|_{i,j,k}^{n}\sin\left(\frac{\omega\Delta t}{2}\right) \tag{2.18}$$

where the central differences were taken. Unfolding the vector product in 2.18 and equalizing the Cartesian components gives a system of three equations in the three unknowns $V\,x, Vy\ and\ Vz$ solvable by imposing the null determinant:

$$\left[\frac{1}{\mathrm{c}\Delta t}\sin\left(\frac{\omega^{\Delta t}}{2}\right)\right]^{2} = \left[\frac{1}{\Delta x}\sin\left(\frac{\mathrm{k^{x\Delta x}}}{2}\right)\right]^{2} + \left[\frac{1}{\Delta y}\sin\left(\frac{\mathrm{k^{y\Delta y}}}{2}\right)\right]^{2} + \left[\frac{1}{\Delta z}\sin\left(\frac{\mathrm{k^{z\Delta z}}}{2}\right)\right]^{2} \tag{2.19}$$

To get the expression for the general theory of numerical dispersion in three dimensions, Equation 2.19 is not normalized about c. It is possible to get k for a one-dimensional electromagnetic wave from 2.19, where two components are cancelled between the three:

$$k^{=\frac{2}{\Delta}}\arcsin\left(\frac{\Delta}{\mathrm{c}\Delta t}\sin\left(\frac{\omega\Delta t}{2}\right)\right) \tag{2.20}$$

It should be noted that spatial resolution has a direct impact on the numerical phase velocity, keeping in mind the relationship between phase velocity and wave number. By wavelength, we determine the cell density:

$$\mathrm{N_y}=\frac{\lambda}{\Delta} \tag{2.21}$$

It serves as a transitional element between a numerical region and the actual electromagnetic environment. According to empirical choice, $Ny = 20$. Therefore, Δmax must not exceed the limit

Δ if we wish to evaluate electromagnetic fields inside of a structure in a specific frequency band. In actual situations, the following prerequisite must be satisfied:

$$\Delta > \frac{\lambda \min}{10} \tag{2.22}$$

The accuracy of the transition improves if $\Delta \max < \Delta$. In fact, if the number of cells increases, the calculation time will also increase. To counteract this increase, the previously defined time step Δt should be reduced. The 2.20 highlights another important parameter: the Courant number.

$$S = \frac{c\Delta t}{\Delta} \tag{2.23}$$

In choosing the time step, criteria must be used to maintain the stability of the system. From 2. 19 solving for ω

$$\tilde{\omega} = \frac{2}{\Delta t} \arcsin\left(\tilde{\xi}\right) \tag{2.24}$$

Where,

$$\tilde{\xi} = c\Delta t \sqrt{\frac{1}{(\Delta x)^2} sin^2\left(\frac{\tilde{k}x\Delta x}{2}\right) + \frac{1}{(\Delta y)^2} sin^2\left(\frac{\tilde{k}y\Delta y}{2}\right) + \frac{1}{(\Delta z)^2} sin^2\left(\frac{\tilde{k}z\Delta z}{2}\right)} \tag{2.25}$$

From 2.25 we get:

$$0 \leq \tilde{\xi} \leq c\Delta t \sqrt{\frac{1}{(\Delta x)^2} + \frac{1}{(\Delta y)^2} + \frac{1}{(\Delta z)^2}} \equiv \xi limite \tag{2.26}$$

The wave vector components that maximize ξ are as follows:

$$\begin{aligned} \tilde{k}y &= \pm \frac{\pi}{\Delta x} \\ \tilde{k}x &= \pm \frac{\pi}{\Delta y} \\ \tilde{k}z &= \pm \frac{\pi}{\Delta z} \end{aligned} \tag{2.27}$$

In case $\xi limitee > 1$ due to Δt the numerical pulsation would be complex. Under these conditions it is possible to prove the instability of the associated numerical system [11]. There stability condition is as follows:

$$\xi limite \leq 1 \tag{2.28}$$

Namely,

$$\Delta t \leq \frac{1}{c\sqrt{\frac{1}{(\Delta x)^2} + \frac{1}{(\Delta y)^2} + \frac{1}{(\Delta z)^2}}} \tag{2.29}$$

For example, for a cubic cell $\Delta x = \Delta y = \Delta z = \Delta$ then:

$$\Delta t \leq \frac{1}{c\sqrt{\frac{1}{(\Delta x)^2} + \frac{1}{(\Delta y)^2} + \frac{1}{(\Delta z)^2}}} = \frac{\Delta}{c\sqrt{3}}$$

$$S = \frac{c}{\Delta} . \frac{\Delta}{c\sqrt{3}} = \frac{1}{\sqrt{1}} \tag{2.30}$$

Exceeding the S value may cause the results to diverge. In this case the program would be wrong since the result would increase until it became so large that it could no longer be represented by a programming language like C. The Courant number is commonly referred to as the stability factor.

2.4 Accuracy of results

There are a few options that will affect how accurate the results are:

- Specification of the programming-related variables.
- Elementary cell size.
- Equalization of the numerical grid; and
- Absorption criteria.

First off, the elementary cell needs to be both large enough to prevent slowing down calculation time and tiny enough to avoid anisotropy and numerical dispersion issues [11]. A reduction in the side of the elementary cel by half in three-dimensional domains results in increases of eight times the memory occupation and sixteen times the calculation time [7]. The electrical properties of the material affect the cell's density. For $\varepsilon, \mu \; and \; \sigma$ values at the same frequency it is necessary to counteract the decrease in λ by reducing the size of the cells.

The real region of calculation cannot be infinite, so when studying open problems, one must virtually limit the space to be considered; in the limiting surfaces, boundary conditions must be imposed that must simulate the removal of incident waves at the boundary of the domain of interest (absorbent conditions). The best known are the ABCs (Absorbing Boundary Conditions) or RBC (Radiation Boundary Conditions); All of them, however, introduce errors, spurious reflections.

These requirements are even more precise the closer the incident field is to the plane in which they are applied and the closer the field becomes a plane wave type structure as it approaches the domain boundary. Recently, absorbent conditions based on a different theory have been proposed. The domain of interest ends with a PML (Perfectly Matched Layer) medium, which has an electrical and magnetic conductivity such that the relative impedance between free space and the medium itself does not change and is always adapted. especially if the medium contains characteristics that:

$$\frac{\sigma}{\varepsilon o} = \frac{\sigma m}{\mu o} \tag{2.31}$$

Therefore, its characteristic impedance is equivalent to that of the vacuum. The reflection at the contact is lowered according to the adaption between the vacuum and the medium. The presence of leaks causes the signal to be muted when it enters the medium. To reflect the signal back inward and cause further attenuation, the domain is terminated with a PEC (Perfect Electrical Conductor) (Figure 2.3).

The conductivity profile can be made to absorb waves at any angle of incidence with respect to the interface by adjusting it along the path of propagation.

The medium in question provides very accurate results, spurious reflections of the order of -60 dB. Most of the computational burden is offset by the fact that with PML conditions they can be placed close to the objects analyzed, allowing a reduction in the overall volume of investigation.

The fundamental constraint is to choose the cell sizes so that they are much smaller than the smallest wavelength for which accurate results are required, i.e. that this size must be less than $\frac{\lambda}{10}$, the ideal would be to have a cell size of $\frac{\lambda}{20}$ to have a good accuracy of the results.

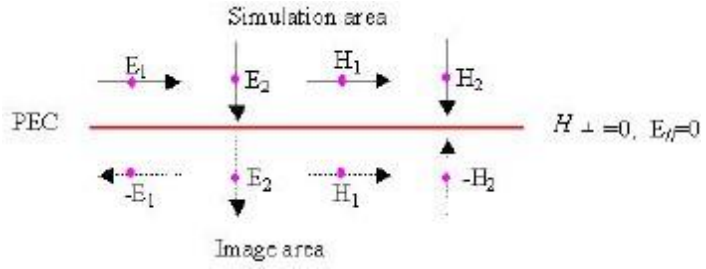

Figure 2.3 PEC field

PMLs offer great accuracy but are challenging to construct and have long processing times [8] [9], whereas the ABC technique of second-order MUR has some computational speed loss. It is crucial to keep in mind that absorption conditions are mathematical constructs that take control of a limited number of cells at the computational domain's extremes to create the FDTD's calculation domain. They have no physical analogue.

Chapter-3

3- Simulation Setup

3.1 Introduction

The aim of this research, to reduce the electromagnetic radiation which penetrating through walls from outdoor environment to indoor environment. Due to increasing of the network band and electronic devices usage in surrounding environments. For this problem we are using the shielding effectiveness by applying the material characteristics in form of code to simulate and find the solution for increasing electromagnetic radiation day-to-day in our life. Here we are simulating the 5 different Layers which act as shielding effeteness to check it propagation and using four different tasks.

3.2 Implementation

For the implementation setup I used the programming language is python. The python is a high-level object-oriented language and easy to learn programmers also and it is the python is a dynamically semantic, object-oriented, high-level, interpreted programming language. Due to its high-level built-in data structures, dynamic typing, and dynamic binding, it is well suited for rapid application development as well as for use as a scripting or glue language to connect existing components. Python's concise syntax places a strong emphasis on readability and ease of use, which decreases the cost of program maintenance. The modularity and reuse of code in programs are encouraged by Python's support for modules and packages. The Python interpreter and the extensive standard library are freely there is no compilation stage, the edit-test-debug cycle is incredibly speedy distributable and are offered in source or binary format for all widely used systems. Python's increased efficiency frequently leads to programmers falling in love with it. Because there is no compilation stage, the edit-test-debug cycle is incredibly speedy. Python programs are easy to troubleshoot because a segmentation failure is never the result of a bug or bad input. Instead, if an error is discovered, the interpreter raises an exception. If the program doesn't handle the exception, the interpreter publishes a stack trace. A source level debugger allows you to set breakpoints, evaluate arbitrary expressions, view local and global variables, step through the code one line at a time, and use other features. The debugger was created in Python, demonstrating the language's capacity for introspection. However, due to the short edit-test-debug cycle enabled by this simple approach, adding a few print lines to the

source code is frequently the fastest way to debug a program. The previously introduced Jupyter notebook s a web-based interactive computing platform. Open -source software for many programming languages. Jupyter Lab is the brand-new web-based user interface for Project Jupyter. You can interact with documents and tasks like Jupyter notebooks, text editors, terminals, and custom components in a flexible, integrated, and extendable way with the help of Jupyter Lab. For an illustration of Jupyter Lab's capabilities. Using splitters and tabs, you can set up several documents and tasks side by side in the workspace. Integration between documents and activities creates new workflows for interactive computing, such as:

- Code Consoles: To enable interactive code execution, offer temporary scratchpads with full support for rich output. It can be used as the notebook's computation log when a code console is connected to it. For example
- Kernel-backed documents enables interactive execution of text-based (Markdown, Python, R, LaTeX, etc.) programs in any Jupyter kernel.
- To create simple dashboards with interactive controls supported by a kernel, notebook cell outputs can be mirrored into their own tab, next to the notebook.
- Live document editing is possible thanks to multiple views of documents in various editors or viewers. For instance, it is simple to view live previews of documents in Vega/Vega-Lite, Markdown, or Delimiter-separated Values. A uniform approach for viewing and manipulating various data formats is also provided by Jupyter Lab.
- It can show rich kernel output in a variety of file formats, including pictures, CSV, JSON, Markdown, PDF, Vega, and Vega-Lite. For more details, see File and Output Formats.
- It is also offering a consistent method for seeing and interacting with different data formats. Rich kernel output can be displayed in Jupyter Lab in a number of file types, including images, CSV, JSON, Markdown, PDF, Vega, and Vega-Lite. See File and Output Formats for more information.
- Jupyter Lab will eventually take the role of the conventional Jupyter Notebook. During this transition, the same notebook document format will continue to be supported by both the conventional Notebook and Jupyter Lab.

Now, using this environment to implement our python code and analysis of shielding effeteness according to layer model which is using for the analysing the effect of electromagnetic field been penetrated outside environment to inside environment.

For simulation we used the five layers of different material's and the first layer (Air), second layer (Teflon), third layer (Cement), fourth layer (Teflon), fifth layer (Air) and this layer's setup act shielding effecting in this project than electromagnetic radiation propagates through these layers and multiple reflections in one single layers. The incident field decreases during the passing of the barrier due to a variety of factors. A portion of the field is reflected in between the layers and now this setup we arrange by using the python code in the environment of jupyter lab to analyse the shielding effeteness.

3.3 Simulation

For simulation I used the multiple layers numerical values to replace the practical experiment for which approximately matches to how they act in the physical environment behaviour. I setup the five layers as the shield combination are air, teflon, cement, teflon and air. Now I started implementing experiment script in the python code and executed in the jupyter-lab environment. Now, started the code by importing three libraries are import scipy. constants as scp, import numpy as np and import matplotlib.ploylot as plt.

Scipy: The library main function is used for common tasks in science and engineering, scipy includes modules for optimization, linear algebra, integration, interpolation, special functions, FFT, signal and image processing, ODE solvers, and other related topics.

Numpy: The equivalent of arrays in Python are lists, although they take a long time to execute. The goal of NumPy is to offer array objects that are up to 50 times faster than conventional Python lists. The NumPy array object is referred to as ndarray, and it has several supporting methods that make using ndarray relatively simple. In data research, where speed and resources are crucial, arrays are employed a lot. In contrast to lists, NumPy arrays are stored in a single continuous location in memory, making it very easy for programs to access and manipulate them. In computer science, this characteristic is known as locality of reference. This is the primary factor that makes numpy faster than lists. Additionally, it is enhanced to function with modern CPU architectures. Although some of the python library numpy is written in python, most of the portions that call for quick computation are implemented in C or C++.

Matplotlib: A description of the pyplot user interface. Please also refer to the quick start guide for a description of matplotlib's functionality and the matplotlib application interfaces (APIs) for a discussion of the trade-offs between the user APIs that are offered. It is a group of procedures that

enable matplotlib to do MATLAB-like operations. Each pyplot function modifies a figure in some way, such as by creating a figure, a plotting region within a figure, some lines within a plotting area, labeling the plot, etc. The plotting functions are directed to the current axes, and various states are retained throughout function calls to keep track of things like the current figure and plotting area (please note that "axes" here and in most places in the documentation refers to the axes part of a figure and not the strict mathematical term for more than one axis). While often less verbose than the explicit API, the implicit pyplot API is also less flexible. Most of the function calls you see above may be made by axes objects as methods. The matplotlib application interfaces document discusses the trade-offs of the supported user APIs. Mu_0 is Permeability the amount of magnetization that a material acquires in electromagnetism in response to an applied magnetic field. A characteristic of a material that can be defined as a relative increase or decrease in the resultant magnetic field inside a material compared to the magnetizing field in which the given material is located, or as the magnetic flux density B established within the material by a magnetizing field divided by the magnetic field strength H of the magnetizing field. Therefore, magnetic permeability has the formula = B/H. The concentration of magnetic field lines, or flux, per unit cross-sectional area, or magnetic flux density, determines the real magnetic field of a material. And then assigned the values to pi, epsilon, mu_0, to execute the values in formula this all are constant as per scipy execution and then i defined the materials of layers with the pi, mu, epsilon and this values a signed to omega now to multiple the frequency with pi and scp this omega will assign to epsilon with respect to the sigma and alfa, beta will be given values of epsilon and omega multiplying with the time and afters this return the gamma and eta to perform the loop cycle and then I defined the snell function. Snell's law is an optical relationship between the refractive indices of the two contacting substances and the path a light ray takes to cross a boundary or surface of separation between them. The Dutch astronomer and mathematician Willebrand Snell made this law known in 1621. At Frist I created the three variables are n1, n2, theta_inc and executed the if and else statement to perform the code according to snell law.

Campi: The common manageability programming interface in c++ language it acts like interface in between wbemserver and wbem (web-based enterprise management) provider Prior to the introduction of CMPI, each WBEM server implementation had its own distinct programming interface for CIM providers. CMPI enables the creation of CIM providers that are largely or completely independent of the type of WBEM server they are used with. As a result, CMPI providers can be integrated across a variety of operating environments with little to no modification work. The

financial commitment to these CIM suppliers is protected in this way. In campi fuction according to code it explains the interface and now I compute the gamma and thick of materials with respect to the layers which used for the experiment. I signed the five layers according to the model which I consider performing the experiment and now implemented all functions in step by step to run and I set the frequency and given start and stop limits and number of points by using the linspcae function then for logic function apply to set range for propagation constant and impedance characteristic. As next step defines the shielding effeteness by using the eta_epsilon and eta_mu0 and states with resepect to the gamma, layers by using the for loops to execute the code. Then started the main code with signing the layers according to our multiple layer model and four different tasks with run with for loops to set the ranges and given thickness with respect to x and y axis in size of 16 and label the x-axis for frequency which is measures in “GHz “and y-axis for shielding effeteness which is measures in “db.” And finally plotted the analysis graph.

Task-1: As per the model first task was performed three layers (Air, Teflon, Air) to observe the shielding effeteness as per the materials.

Task-2: As per the model second task was performed three layers (Air, Cement, Air) to observe the shielding effeteness as per the materials.

Task-3: As per the model second task was performed four layers (Air, Teflon, Cement, Air) to observe the shielding effeteness as per the materials.

Task-4: As per the model second task was performed five layers (Air, Teflon, Cement, Teflon, Air) to observe the shielding effeteness as per the materials.

3.4 Python Code:

```
import scipy.constants as scp
import numpy as np
import matplotlib.pyplot as plt
%matplotlib inline
import matplotlib_inline.backend_inline
matplotlib_inline.backend_inline.set_matplotlib_formats('svg')pi=scp.pi
eps0=scp.epsilon_0
mu0=scp.mu_0
c=scp.c
print("sciPy - pi = %.16f"%pi)
```

```
print("sciPy - eps0 = %.16g"%eps0)
print("sciPy - mu0 = %.16g"%mu0)
print("sciPy - c = %.1f"%c)
```

```
sciPy - pi = 3.1415926535897931
sciPy - eps0 = 8.854187812800001e-12
sciPy - mu0 = 1.25663706212e-06
sciPy - c = 299792458.0
```

```
def materiale (strato):
epsr=strato[1]
mur=strato[2]
sigma=strato[3]
omega=2*scp.pi*freq
epsr2=sigma/(omega*scp.epsilon_0)
tgd2=(epsr2**2)/(epsr**2)
alfa=omega * np.sqrt (mur * scp.mu_0 * epsr * scp.epsilon_0 * 0.5 * (np.sqrt (1 + tgd2) - 1))
beta=omega * np.sqrt (mur * scp.mu_0 * epsr * scp.epsilon_0 * 0.5 * (np.sqrt (1 + tgd2) + 1))
gamma=alfa + beta * 1j
eta=np.sqrt (mur * scp.mu_0 / ((epsr - epsr2 * 1j) * scp.epsilon_0))
return gamma, eta
def interf (e1,e2):
eta1=e1
eta2=e2
rho = (eta2-eta1)/(eta2+eta1)
tt = 1 + rho
return rho, tt
def campi (gamma, thick, rho, tt, e_p, e_m):
gamma=gamma
thick=thick
e_p=e_p
e_m=e_m
rho=rho
tt=tt
exp_piu = np.exp (gamma * thick)
```

```
exp_meno = np.exp (- gamma * thick)
e_piu = (exp_piu * e_p + rho * exp_meno * e_m) / tt
e_meno = (rho * exp_piu * e_p + exp_meno * e_m) / tt
return e_piu, e_meno
def SE(freq):
for i in range(nstrati):
gamma[i],eta[i]=materiale(strati[i])
for i in range(nstrati-1):
rho[i],tt[i]=interf(eta[i],eta[i+1])
i=nstrati-1
e_p[i] = 1 + 0j;
e_m[i] = 0 + 0j;
for i in range(nstrati-2, -1, -1):
e_p[i], e_m[i] = campi (gamma[i+1], strati[i+1][4], rho[i], tt[i], e_p[i+1], e_m[i+1])
return 20 * np.log10(np.abs(e_p[0]))
nstrati=5
gamma=[0]*nstrati
eta=[0]*nstrati
tt=[0]*(nstrati-1)
rho=[0]*(nstrati-1)
e_p=[0]*(nstrati)
e_m=[0]*(nstrati)
#strati = [("aria 1",1,1,0,0),
#         ("vetro 1",7,1,0.001,0.008264),
#         ("metallo",1,1,61730000,6.5e-9),
#         ("aria 2",1,1,0,0.01218),
#         ("vetro 2",7,1,0.001,0.003615),
#         ("aria 3",1,1,0,0)]
#
strati=[("aria 1",1,1,0,0),
("Teflon 1",2.8,1,0.001,0.008264),
("cement",3.2,3.6,0.4,1e-2),
```

```
("Teflon 2",2.8,1,0.001,0.004),
("aria 2", 1,1,0,0)]
#freq=1e9
freq = np.linspace ( start = 100e6    # lower limit (Hz)
, stop = 10e9      # upper limit (Hz)
, num = 501      # generate 501 points between 0 and 3
)
for i in range(nstrati):
gamma[i],eta[i]=materiale(strati[i])
#print("Materiale:",strati[i][0]," - Costante di propagazione =",np.round(gamma[i],2),"(1/m),
Impedenza caratteristica =",np.round(eta[i],2),"ohm")
for i in range(nstrati-1):
rho[i],tt[i]=interf(eta[i],eta[i+1])
#print("Interfaccia:",i," - Coefficiente di trasmissione =",np.round(tt[i],5)," Coefficiente di
riflessione =",np.round(rho[i],5))
i=nstrati-1
e_p[i] = 1 + 0j;
e_m[i] = 0 + 0j;
#print("Materiale:",strati[i][0]," - E progressivo =",np.round(e_p[i],2),"(V/m), E regressivo
=",np.round(e_m[i],2),"V/m")
for i in range(nstrati-2, -1, -1):
e_p[i], e_m[i] = campi (gamma[i+1], strati[i+1][4], rho[i], tt[i], e_p[i+1], e_m[i+1])
#print("Materiale:",strati[i][0]," - E progressivo =",np.round(e_p[i],2),"(V/m), E regressivo
=",np.round(e_m[i],2),"V/m")
#print("SE (dB) = ", np.round(20 * np.log10(np.abs(e_p[0])),2))
#fstart = 0.1  # IN GHz
#fstop = 10  # IN GHz
#fstep = 1e-3  # IN GHz
#fnum = (fstop - fstart) / fstep + 1
y = SE(freq)    # This is already vectorized, that is, y will be a vector!
#print("x = ",x)
#print("y = ",y)
```

```
plt.rc('xtick', labelsize=16)
plt.rc('ytick', labelsize=16)
plt.rc('axes', labelsize=16)
plt.xlabel('Frequency (GHz)')
plt.ylabel('SE (dB)')
plt.plot(freq*1e-9, y)
plt.grid()
plt.title('fourth analysis( Air,Teflon1,cement,Teflon2,Air)')
plt.savefig('fourth analysis( Air,Teflon1,cement,Teflon2,Air)')
plt.show()
```

```
%whos
Variable          Type       Data/Info
-----------------------------------------
SE                function   <function SE at 0x7f013cac30d0>
c                 float      299792458.0
campi             function   <function campi at 0x7f013ca57e50>
e_m               list       n=5
e_p               list       n=5
eps0              float      8.8541878128e-12
eta               list       n=5
freq              ndarray    501: 501 elems, type `float64`, 4008 bytes
gamma             list       n=5
i                 int        0
interf            function   <function interf at 0x7f013ca57550>
materiale         function   <function materiale at 0x7f013ca57a60>
matplotlib_inline module     <module 'matplotlib_inlin<...>tlib_inline/__init__.py'>
mu0               float      1.25663706212e-06
np                module     <module 'numpy' from '/op<...>kages/numpy/__init__.py'>
nstrati           int        5
pi                float      3.141592653589793
plt               module     <module 'matplotlib.pyplo<...>es/matplotlib/pyplot.py'>
rho               list       n=4
scp               module     <module 'scipy.constants'<...>y/constants/__init__.py'>
strati            list       n=5
tt                list       n=4
y                 ndarray    501: 501 elems, type `float64`, 4008 bytes
```

Chapter-4

4.1-Results

Electromagnetic radiation which is penetration from outdoor environment to indoor environment the reflection and transmission takes place, and these reflections and transmissions will pass through the multiple layers which acts shielding effeteness. For experiment chosen five layers and four different tasks were performed by using these five layers to observe the shielding effeteness will be reduce the electromagnetic radiation which is passing through the layers.
Four different tasks are:

Task-1: The first analysis is using the three layers (Air, Teflon, Air) as shielding effeteness analysing with frequency 10 GHz. This output we observe in figure-(4.1).

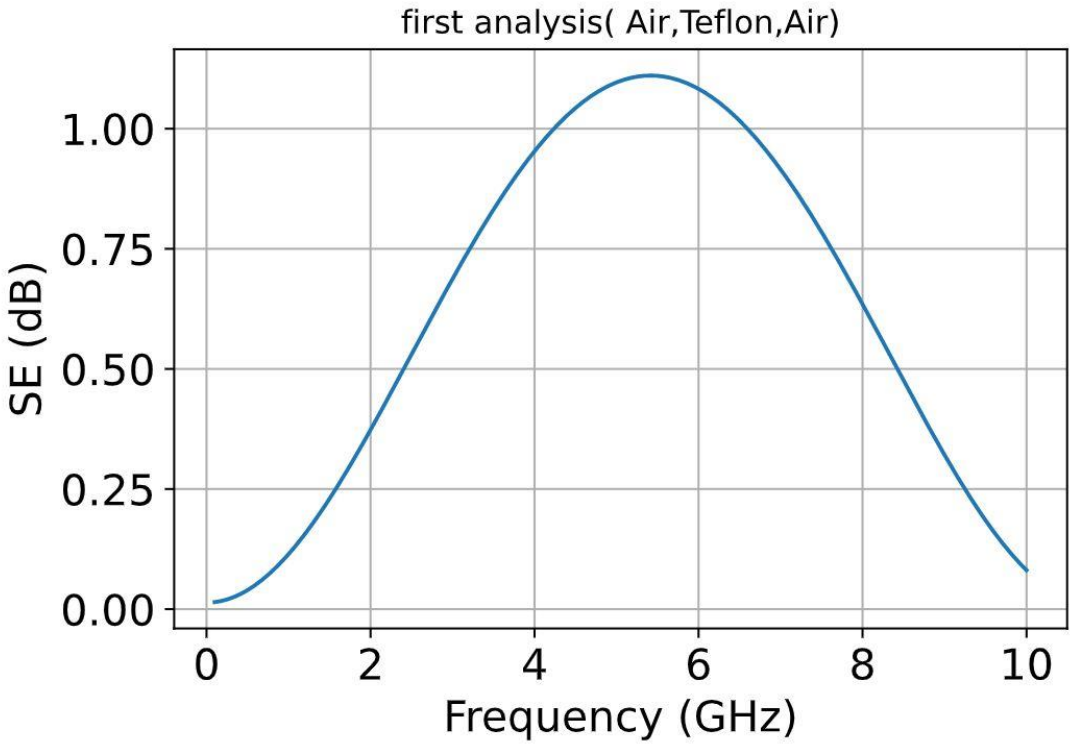

Figure (4.1): x-label shows the frequency (GHz), y-label shows the shielding effeteness (dB) and blue line shows that effect of shielding effeteness according to frequency of radiation.

According to the analysis of first task, the frequency range (5 to 5.5) is observed high effect of shielding effeteness due to Teflon as medium level of permittivity, permeability, conductivity, and Air as low-level of permittivity, permeability and conductivity compared to other materials that means the radiation is observed more in this ranges due the materials used.

Task-2: The second analysis is using the three layers (Air, Cement, Air) as shielding effeteness with frequency 10 GHz. This output we observe in figure-(4.2).

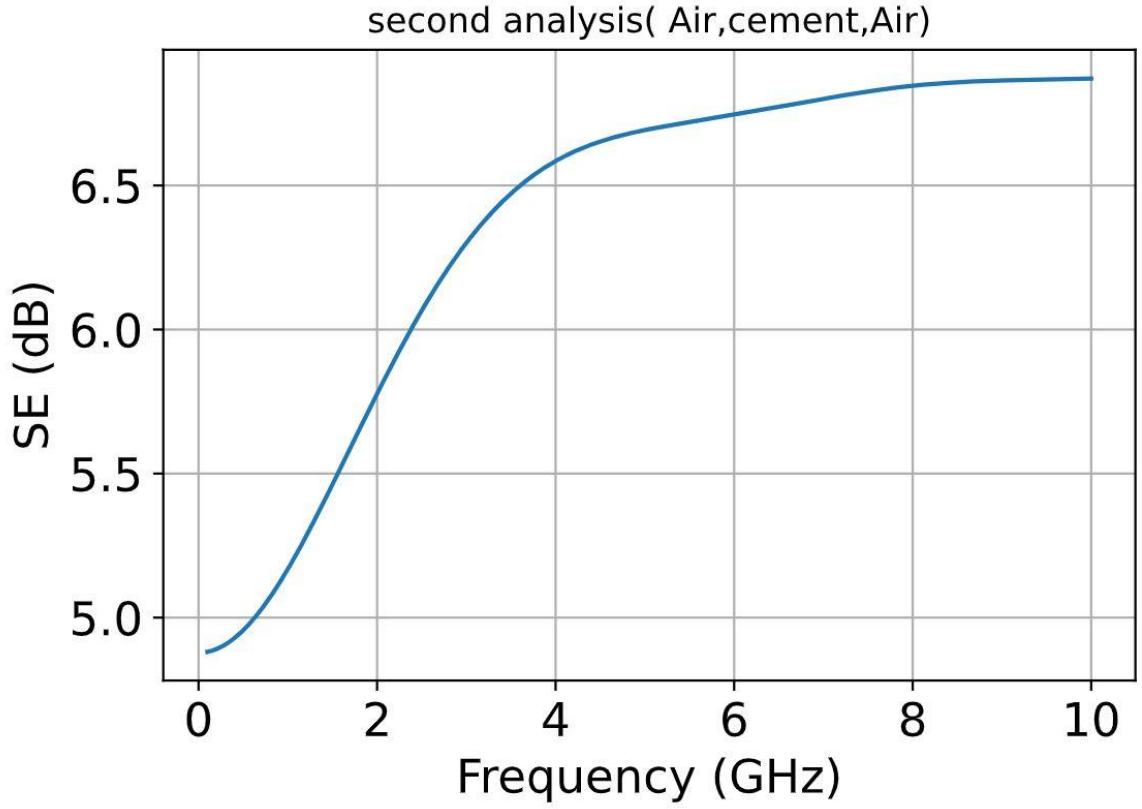

Figure (4.2): x-label shows the frequency (GHz), y-label shows the shielding effeteness (dB) and blue line shows that effect of shielding effeteness according to frequency of radiation.

According to the second task, the frequency range (4-10) is observed high effecting of shielding effeteness due to Cement as high level of permittivity, permeability, conductivity, and Air as low-level of permittivity, permeability and conductivity compared to other materials that means the radiation is observed more in this ranges due the materials used.

Task-3: The third analysis is using the four layers (Air, Teflon, Cement, Air) as shielding effeteness with frequency 10 GHz. This output we observe in figure-(4.3).

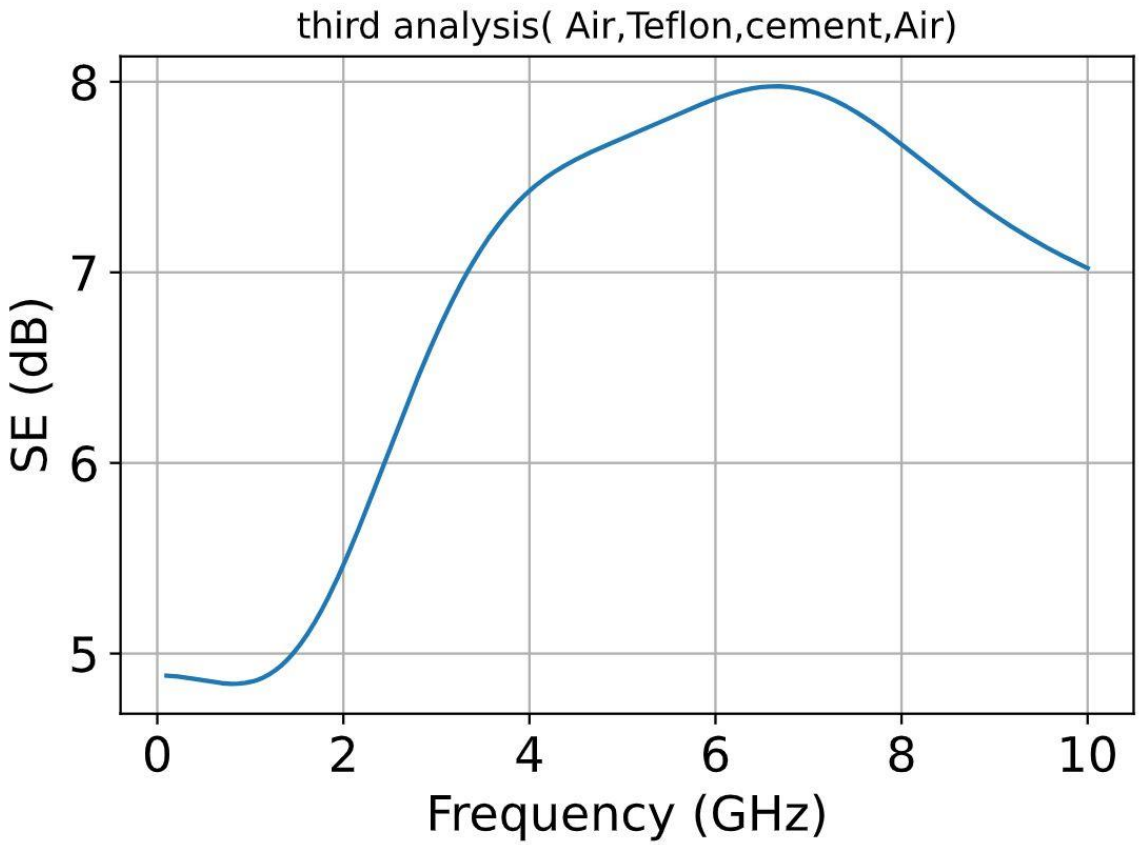

Figure (4.3): x-label shows the frequency (GHz), y-label shows the shielding effeteness (dB) and blue line shows that effect of shielding effeteness according to frequency of radiation.

According to the third task, the frequency range (6-8) is observed high effecting of shielding effeteness due to Cement as high level of permittivity, permeability, conductivity, Teflon as medium level of permittivity, permeability, conductivity, and Air as low-level of permittivity, permeability and conductivity compared to other materials that means the radiation is observed more in this ranges due the materials used.

Task-4: The fourth analysis is using the five layers (Air, Teflon, Cement, Teflon, Air) as shielding effeteness with frequency 10 GHz. This output we observe in figure-(4.4).

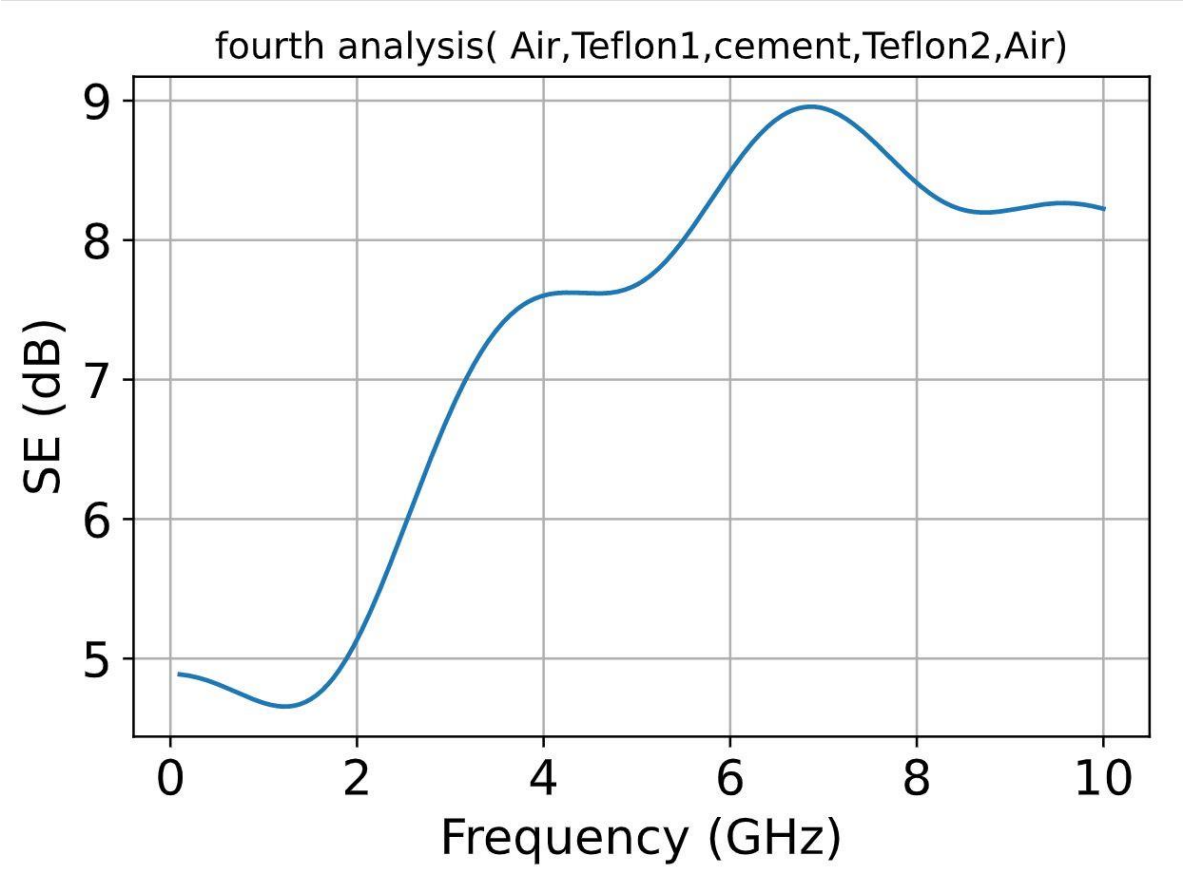

Figure (4.4): x-label shows the frequency (GHz), y-label shows the shielding effeteness (dB) and blue line shows that effect of shielding effeteness according to frequency of radiation.

According to the task, the frequency range (6-8) is observed high effecting of shielding effeteness due to Cement as high level of permittivity, permeability, conductivity, Teflon as medium level of permittivity, permeability, conductivity, and Air as low-level of permittivity, permeability and conductivity compared to other materials that means the radiation is observed more in this ranges due the materials used.

CHAPTER-5
5.1-DISCUSSION

The main objective of the used study was to develop a model for shielding effeteness that considers the various parameters affecting. to reduce the electromagnetic radiation which penetrating through walls from outdoor environment to indoor environment. Due to increasing of the network band and electronic devices usage in surrounding environments. The expression of shielding efficiency may be broken down into three parts, each of which represents the phenomena of loss by reflection, loss by repeated reflections, and loss by absorption. To obtain a quantitative definition, consider a metal barrier (shield) of thickness t, conductivity σ, relative electrical permittivity ε_r and relative magnetic permeability μ_r. Now, for implementations the model used the high-level object-oriented language is python. It is easy to troubleshoot because a segmentation failure is never the result of a bug or bad input. there is no compilation stage, the edit-test-debug cycle is incredibly speedy. if an error is discovered, the interpreter raises an exception. A source level debugger allows you to set breakpoints, evaluate arbitrary expressions, view local and global variables, step through the code one line at a time, and use other features. The debugger was created in Python, demonstrating the language's capacity for introspection. Jupyter lab environment using to implement our python code and analysis of shielding effeteness according to layer model which is using for the analysing the effect of electromagnetic field been penetrated outside environment to inside environment. And materials used for the shielding effeteness are air, Teflon, cement. These materials are arranged in multilayers with respect to thickness and length. For simulating this model, we considered the permittivity, permeability, conductivity, and thickness of the layers. Then implementation in form python code for this imported some functions which supports to run logic which required for the model implementation and chosen function are SciPy. Constants as scp, NumPy. as np, matplotlib. pyplot as plt for support to execute the code in jupyter environment. Now performed four task to observe the shielding effeteness works according to number of layers and thickness of materials for this model Used three materials (Air, Cement, Teflon), in first task used three layers (Air, Teflon, Air), second task used three layers (Air, Cement, Air), third task used four layers (Air, Teflon, Cement, Air), Fifth task used five layers (Air, Teflon, Cement, Teflon, Air). According to four task we can observe shielding effeteness is keep on increases when the electromagnetic radiation intensity keeps on incident in high range on the layers.

CHAPTER-6

6.1-CONCLUSION

In conclusion, the electromagnetic radiation analysis, the multiple layers act like shield can be used to carry out tests such as emission tests due to effect of electromagnetic waves passes through the outdoor environment to indoor environment. The incident field decreases during the passing of the barrier due to a variety of factors. A portion of the field is reflected, and this portion is dependent on the material's coefficient of reflection. To obtain a quantitative definition, consider a barrier (shield) of thickness t, conductivity σ, relative electrical permittivity ε_r and relative magnetic permeability μ_r. Now, for implementations the model used the high-level object-oriented language is python. It is easy to troubleshoot because a segmentation failure is never the result of a bug or bad input. The debugger was created in Python, demonstrating the language's capacity for introspection. Jupyter lab environment using to implement our python code and analysis of shielding effeteness according to layer model which is using for the analysing the effect of electromagnetic field been penetrated outside environment to inside environment. According to four task we can observe shielding effeteness is keep on increases when the electromagnetic radiation intensity keeps on incident in high range on the layers.

CHAPTER-7
BIBILOGRAPHY

[1] Clayton R. Paul, “Introduction to Electromagnetic Compatibility” Hoboken (USA): John Wiley & Sons. Inc, 1992, Mexico Documents, 2014.

[2] M. O. Hatfield, J. L. Bean, G. J. Freyer, and D. Johnson, “Repeatability of mode-stirred chamber measurements”, in IEEE International Symposium on Electromagnetic Compatibility, vol. 1, Chicago, IL, USA, August 1994, pp. 485–490.

[3] C. L. Holloway, D. A. Hill, J. Ladbury, G. Koepke, R. Garzia, “Shielding Effectiveness Measurements of Materials Using Nested Reverberation Chambers” in IEEE Transactions on Electromagnetic Compatibility, v. 45, n. 2, pp. 350–356, May 2003.

[4] D. A. Hill, M. T. Ma, A. R. Ondrejka, B. F. Riddle, M. L. Crawford, and R. T. Johnk, "Aperture excitation of electrically large, lossy cavities," in IEEE Transactions on Electromagnetic Compatibility, vol. 36, no. 3, pp. 169-178, Aug. 1994, doi: 10.1109/15.305461.

[5] M. Sadiku, Numerical Techniques in Electrodynamics, 2nd ed. Boston Artech House, 2000.

[6] A. Taflove and M. Brodwin, “Numerical solution of steady-state electromagnetic scattering problems using the time-dependent maxwell’s equations,” IEEE Transactions on Microwave Theory and Techniques, vol. 23 (8):623-630, aug 1975.

[7] J. Fang, Time Domain Finite Difference Computation for Maxwell’s Equations. University of California Berkeley: PhD thesis, 1989.

[8] B. Engquist and A. Majda, “Absorbing boundary conditions for the numerical simulation of waves,” Mathematical Computations, pp. 629–651, 1977.

[9] E. L. Lindman, “Free-space boundary conditions for the time dependent wave equation,” Journal of Computational Physics, pp. 67–78, 1975.

[10] K. S. Yee, “Numerical solution of initial boundary value problems involving maxwell’s equations in isotropic media,” IEE Transactions on Antennas and Propagation, vol. 14 (4):302-307, 1966.

[11] A. Taflove and S. C. Hagness, “Computational electrodynamics: The finite difference time-domain method,” 2000.

[12] Electromagnetic compatibility (EMC) - Part 4-21: Testing and measurement techniques-Reverberation chamber test methods, 2nd ed., International Standards - IEC 61000-4-21, Geneva, Switzerland, Apr. 2011.

[13] F. Moglie and A. P. Pastore, "FDTD analysis of plane wave superposition to simulate susceptibility tests in reverberation chambers," in IEEE Transactions on Electromagnetic Compatibility, vol. 48, no. 1, pp. 195-202, Feb. 2006, doi: 10.1109/TEMC.2006.870793.

[14] F. Moglie, “Convergence of the reverberation chambers to the equilibrium analysed with the finite-difference time-domain algorithm,” vol. 46, no. 3, pp. 469–476, Aug. 2004.

[15] Tesche, Frederick M., M. Ianoz, and Torbjörn Karlsson. EMC Analysis Methods and Computational Models. New York: John Wiley & Sons, 1997.

[16] “Shielding Design Methodology & Procedures by Donald R. J. White”.

[17] https://ieeexplore.ieee.org/document/9559283.

[18] https://ieeexplore.ieee.org/document/8879274.

[19] https://ieeexplore.ieee.org/document/8495326.